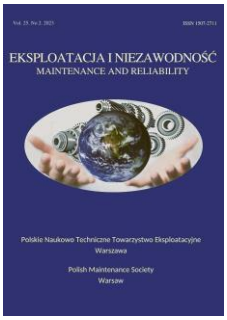

Eksploatacja i Niezawodnosc – Maintenance and Reliability

Volume 28 (2026), Issue 3

journal homepage: http://www.ein.org.pl

Article citation info:
Yan Y, Wang P, Li L, Reliability evaluation of lifting machinery electronic equipment: a progressive framework from testing, data analysis to assessment, Eksploatacja i Niezawodnosc – Maintenance and Reliability 2026: 28(3) http://doi.org/10.17531/ein/218671

Reliability evaluation of lifting machinery electronic equipment: a progressive framework from testing, data analysis to assessment

Indexed by: Web of Science Group

Yabin Yan[a,b,*], Pengbin Wang[a], Lei Li[c]

[a] School of Electrical and Intelligent Manufacturing, Jiangsu Normal University Kewen College, China
[b] School of Information and Control Engineering, China University of Mining and Technology, China
[c] Xuzhou Heavy Machinery Co., Ltd., China

Highlights

- The systematic assessment framework aligns closely with engineering requirements.
- The practical model integrates PoF to overcome data scarcity and poor interpretability.
- The assessment algorithm enables real-time RUL prediction, rapid and straightforward deployment.

Abstract

Reliability of electronic equipment is critical for lifting machinery safety. Studies have primarily concentrated on electronic components with limited attention to holistic frameworks. This paper proposes a reliability evaluation methodology for electronic equipment, addressing key limitations in systematic frameworks and practical utility. First, accelerated life test (ALT) is designed according to Coffin-Manson model, amplifying environmental stress to degradation. Second, wavelet packet (WP) is employed to extract performance degradation trends, enhancing data quality for subsequent analysis. Third, a pseudo-lifetime estimation approach is developed based on autoregressive moving average (ARMA) and performance degradation trajectory. Weibull distribution model is then used for quantitative reliability analysis. Finally, reliability test and analysis of load moment limiter (LML) demonstrate that the methodology is efficient, precise, and practically implementable, thereby bridging the gap between academic research and field applications.

Keywords
reliability assessment, ALT, WP, performance degradation trajectory, electronic equipment, lifting machinery

1. Introduction

Lifting machinery is widely employed in building, transportation, and industrial manufacturing. Electronic equipment serves as the core platform for operation control, safety monitoring, and information exchange. With advances in semiconductor technology, it has become increasingly critical to lifting machinery. The reliability of electronic equipment is crucial to production safety, asset security, and personnel safety, as its malfunction can lead to operational disruption and even safety incidents. Consequently, reliability research is fundamental to fault prediction and preventive maintenance.

In recent years, research on semiconductor reliability has emerged as a frontier topic in academia. Owing to the superior material properties, wide-bandgap semiconductors (WBG) such as silicon carbide (SiC) and gallium nitride (GaN), are gradually replacing conventional silicon-based components. The unique failure mechanisms associated with WBG devices have become central to reliability studies. For SiC metal oxide semiconductor field effect transistors (MOSFETs), key reliability concerns include gate-oxide integrity, short-circuit robustness, and the stability of Drain-Source On-Resistance [1,2]. In the case of

(*) Corresponding author.
E-mail addresses: Y. Yan (ORCID: 0009-0008-3943-0303) ybyan@cumt.edu.cn, P. Wang (ORCID: 0009-0009-5060-1123) wangpengbin906@gmail.com, L. Li (ORCID: 0009-0005-9548-112X) li_lei2006@126.com

GaN high-electron-mobility transistors (HEMTs), dominant reliability bottlenecks involve threshold voltage instability and current collapse [1,3]. These failure mechanisms are closely linked to material defects and thermomechanical stresses experienced during operation. Extensive reliability research has been conducted on the electronic components associated with these semiconductors (e.g., insulated gate bipolar transistors (IGBTs) [4–7]). Meanwhile, system miniaturization has been achieved through high-density integration with the development of heterogeneous integration and package technology. The reliability of package is increasingly influenced by thermal management [8]. The non-component-level failure mechanisms directly compromise electronic equipment lifespan, such as printed circuit board (PCB) cracking and solder joint fatigue failure that manifest themselves progressively due to cumulative thermal cycling impacts [9]. Existing research has also demonstrated that the primary vulnerability of electronic equipment has shifted from component-level defects to interconnect failure encompassing solder joints and plated through-holes [10]. Consequently, equipment-level reliability is equally critical for academic research, and needs particular attention [11,12]. Importantly, this perspective aligns closely with manufacturers' strategic priorities, particularly their emphasis on enhancing equipment-level reliability and implementing preventive maintenance protocols.

Moreover, reliability research is primarily focused on application domains such as avionics, power electronics, and automotive electronics. In aerospace applications, electronic equipment is subjected to extreme environmental stresses, including wide temperature swings, thermal cycling, and ionizing radiation. The reliability of spacecraft electronic equipment in such harsh environments was investigated in [10], providing a foundation for avionics design. CHEN et al. [13] developed a reliability model for avionic systems based on cumulative damage theory, providing guidance for quantitative reliability evaluation and design optimization. Xu et al. [14] suggested a hierarchical reliability modeling and assessment framework for More Electric Aircraft, with dedicated focus on electronic components, subsystems, and system-level. MIL-HDBK-217 [15], RIAC [16], and FIDES [17] are reliability assessment approaches for photovoltaic inverters and other typical power electronic components. Anusuya K. et al. [18] established a reliability evaluation framework for photovoltaic inverters through comparative analysis of these three approaches. Additional advanced methods include Monte Carlo simulation [19], failure data-driven machine learning [20], and stress-strength analysis [21]. In the field of automotive electronics, GM Company standard GMW3172 and industry standard IPC-A-610GA are adopted along with their integrated adaptations [22]. Although reliability research in these domains provides a reference for electronic equipment in lifting machinery, the latter still lacks industry-standardized, widely accepted reliability assessment methodologies that are technically rigorous and practically implementable in engineering.

In addition, as a typical type of special-equipment, lifting machinery poses significant reliability research challenges under small-sample constraints. Researchers have primarily adopted strategies such as generative models, metric-based meta-learning, and regularization techniques to address this issue. The generative models approach leverages a data-driven strategy to synthesize or simulate lifetime data, serving as a form of data generation and enhancement [23]. Metric-based meta-learning constructs transferable metric spaces that enable models to rapidly adapt to new tasks using only a few labeled samples [24]. Regularization techniques, widely employed to mitigate model overfitting, have also been integrated into small-sample learning frameworks [25]. Despite these advances, significant limitations hinder their practical application to electronic equipment in lifting machinery. First, a lack of physical interpretability prevents these "black-box" models from revealing the underlying mechanisms by which environmental stressors drive performance degradation and failure. Second, existing approaches exhibit high sensitivity to data quality [26]. In the context of lifting machinery, reliability data are typically expensive to acquire, incomplete, and highly heterogeneous in quality. Models trained on such noisy and sparse datasets yield lifetime predictions with substantial uncertainty, and are insufficient for informed engineering decisions. Third, limited generalizability remains a critical barrier. Models trained on domain-specific datasets cannot be transferred to lifting machinery electronics, or be deployed offline to provide users with real-time remaining useful life (RUL) prediction.

In general, reliability research for electronic equipment in lifting machinery is constrained by the lack of equipment-level, standardized, and practically viable small-sample predictive approaches that can be seamlessly integrated into engineering workflows. This paper makes three key contributions:

1. Systematic assessment framework. A comprehensive reliability evaluation methodology-integrating ALT, data analysis, and quantitative assessment algorithm-is systematically proposed for lifting machinery electronic equipment. It addresses equipment-level failure mechanisms beyond individual components. Additionally, the procedural design of this methodology aligns closely with practical engineering requirements, which explicitly prioritize standardization and deployability.

2. Practical applicability. The methodology enables reliability assessment under small-sample constraints. After preprocessing the ALT data based on WP, we introduce a performance degradation framework that integrates physics-of-failure (PoF) mechanisms to mitigate data scarcity and overcome poor interpretability inherent in existing "black-box" models. Moreover, the constructed degradation model exhibits generalizability across similar electronics, facilitating standardized implementation by manufacturers.

3. Certifiable accuracy algorithm. An assessment algorithm leveraging time-series performance degradation is developed, with accuracy certifiable through comparative validation. And this approach enables real-time RUL prediction and preventive maintenance without requiring offline learning redeployment.

2. Experiment design and data analysis

2.1. ALT method

Due to high reliability design, traditional life testing fails to generate sufficient failure data for electronic equipment. ALT addresses this limitation by applying elevated stress levels to substantially reduce test duration, thereby enhancing efficiency and lowering costs [27–29]. It is particularly suitable for lifting machinery electronic equipment. As the essence of ALT, acceleration models include Arrhenius model, Eyring model, Generalized Eyring model, and Coffin-Manson model [17,28]. These models characterize the relationship between equipment lifespan and various stress factors, such as temperature, humidity, and vibration, with temperature identified as the dominant influence [9,10,30].

In electronic equipment, the interaction of thermal stress and creep leads to the formation of coarse stripe-like structures and voids within internal solder joints. These stripe-like structures and voids continuously expand or gradually coalesce into microcracks during temperature cycles, ultimately resulting in solder joint failure. The Coffin-Manson model delineates the correlation between temperature cycle and lifespan by utilizing the disparities in thermal expansion coefficients among various materials. It amplifies the detrimental impact of thermal stress induced by temperature fluctuation. Furthermore, compared to other models, ALT based on Coffin-Manson model requires fewer samples. Consequently, ALT can be formulated for lifting machinery electronic equipment with the following essential elements:

(1) Coffin-Manson model

$$A_{\mathrm{CM}} = \left(\frac{\Delta T_{\mathrm{t}}}{\Delta T_{\mathrm{F}}}\right)^{c} \tag{1}$$

where, A_{CM} is acceleration factor, c represents Coffin-Manson index, ΔT_{t} represents mean temperature difference, and ΔT_{F} denotes difference between the maximum and minimum temperatures within a temperature profile, i.e.

$$\Delta T_{\mathrm{t}} = T_{\max} - T_{\min} \tag{2}$$

where $T_{\max}$ and $T_{\min}$ denote top and low limit of temperature, respectively.

(2) Thermal stress profile

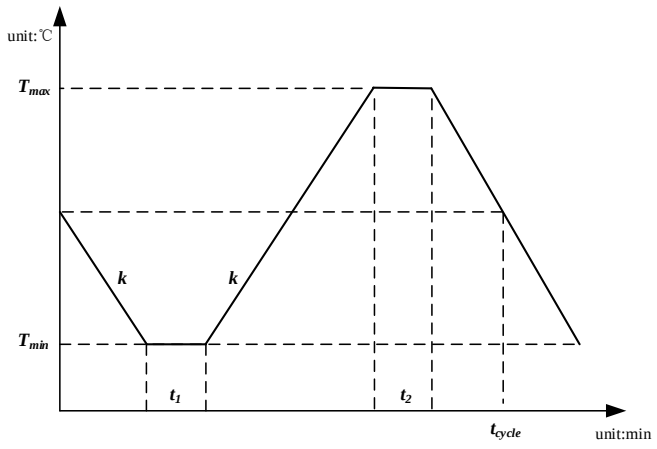

Figure 1. Thermal stress profile of ALT.

In Fig. 1, k denotes the rate of temperature change, t_1 and t_2 represent the dwell time at minimum and maximum temperature, respectively. t_{cycle} represents temperature cycling

period, expressed as

$$t_{cycle} = \frac{2*(T_{\max}-T_{\min})}{k} + t_1 + t_2 \quad (3)$$

2.2. Test data analysis method

To address the challenge of extracting features from limited and noisy ALT data, WP is used as an advanced signal analysis technique [31–33]. WP employs a pair of interrelated low-pass and high-pass filters to decompose the signal sequence into low-frequency and high-frequency components at a given scale. It then iteratively decomposes both components at progressively refined scales, yielding a more detailed time–frequency representation. This enhanced resolution enables the precise extraction of signal features embedded within noise.

For the ALT data of lifting machinery electronic equipment, the following procedure is adopted:

(1) Decomposition

ALT data is recursively decomposed based on wavelet transform (see Eq. (4)), yielding a frequency decomposition tree as illustrated in Fig. 2.

$$W_f(a,b) = \frac{1}{\sqrt{|a|}}\int_{-\infty}^{\infty} f(t)\psi^*\left(\frac{t-b}{a}\right)dt \quad (4)$$

where $f(t)$ denotes the analyzed signal, a is scale parameter (inversely related to frequency), and b is translation parameter. The function $\psi(t)$ is mother wavelet, and $\psi^*(t)$ denotes its complex conjugate. The mother wavelet satisfies:

$$C_\psi = \int_{-\infty}^{\infty} \frac{|\hat{\psi}(\omega)|^2}{|\omega|} d\omega < \infty \quad (5)$$

where $\hat{\psi}(\omega)$is Fourier transform of $\psi(t)$, and it is generally required that $\hat{\psi}(0) = 0$.

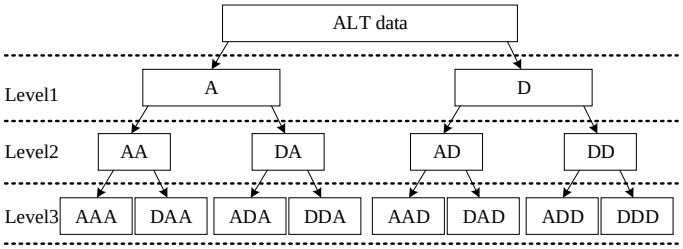

Figure 2. Frequency decomposition tree of WP.

In Fig. 2, the letter A denotes the low-frequency component of ALT data, and D denotes the high-frequency component. Level 1, Level 2, and Level 3 correspond to the first, second, and third levels in WP decomposing, respectively.

(2) Denoising

Noise components are identified and suppressed through thresholding-based strategies [34].

(3) Reconstruction

A denoised version of ALT data is synthesized via inverse wavelet transform (see Eq. (6)).

$$f(t) = \frac{1}{C_\psi}\int_0^\infty \int_{-\infty}^{\infty} W_f(a,b)\psi\left(\frac{t-b}{a}\right)\frac{dbda}{a^2} \quad (6)$$

Based on this procedure, WP effectively suppresses noise induced by test instrumentation, environment during ALT, while retaining degradation-related features essential to reliability assessment. Notably, WP processing can enhance data quality and effectively mitigate the sample sparsity inherent in small-sample reliability studies.

3. Reliability assessment algorithm

3.1. Pseudo-Lifetime

(1) ARMA model

ARMA model constructs a mathematical framework to approximate the behavior of existing time series data. It achieves predictions under the minimum variance criterion by analyzing the inherent structure of dynamic data [35]. The model is denoted by:

$$\sum_{i=0}^{p} \varphi_i Y_{t-i} = \sum_{j=0}^{q} \theta_j \varepsilon_{t-j} \quad (7)$$

where Y_t denotes stationary, nonrandom time series, p is autoregressive order, φ_{i} denotes autoregressive term coefficient, q is moving average order, θ_{j} denotes moving average term coefficient, and $\varepsilon_{\mathrm{t-j}}$ is white noise series.

Based on the ARMA model, failure cycles (n) of test samples can be predicted according to qualified value. Lifespan (L, unit: year) of the sample is subsequently estimated using following equation (8):

$$L = \frac{n \cdot A_{CM}}{N \cdot 365} \quad (8)$$

where N represents mean daily count of temperature variations, *N=2*. L is usually named pseudo-lifetime, because it does not correspond to the actual failure time of electronic equipment.

(2) Performance degradation trajectory

Failure data of electronic equipment are rarely obtainable within short timeframes, presenting significant limitations for failure-based reliability analysis methods. Degradation-based reliability method offers a viable alternative by leveraging the inherent correlations between failure and performance

degradation [14,36], where the degradation process progressively induces cumulative damage effects that ultimately lead to failure.

Performance degradation trajectory of electronic equipment is modeled as:

$$log(y) = \alpha + \beta \hat{t} \quad (9)$$

where y denotes the quantifiable degradation data based on WP, which can be selected according to the characteristics of electronic equipment; α and β are unknown parameters to be identified based on least squares fitting, $\hat{t}$ is time or cycle index of data acquisition; and log() is natural logarithm. It follows that failure cycles (n) can be calculated from the performance degradation trajectory and failure threshold. Pseudo-lifetime of each sample is subsequently derived from Eq. (8).

Eq. (9) is commonly referred to as a concave degradation model. Its mathematical form closely aligns with the performance degradation in electronic equipment subjected to ALT. As the test progresses, thermal fatigue and similar dominant failure mechanisms govern the aging behavior. This physical phenomenon is precisely captured by the concave functional form [37,38]. Consequently, Eq. (9) constitutes a physically consistent and meaningful abstraction of the underlying degradation mechanisms in lifting machinery electronic equipment.

(3) Comparative analysis of ARMA model and performance degradation trajectory

While ARMA model provides effective linear parametric analysis of dynamic data, its parameters remain purely statistical abstractions without physical significance. Additionally, because lifting machinery is classified as special-equipment, ALT is constrained by practical factors, that include high testing costs, long experimental cycles, and production scheduling. These factors result in a small number of available test samples and scarcity of ALT data, which fundamentally limit the applicability and performance of ARMA model.

In contrast, performance degradation trajectory integrates PoF mechanisms and inherently establishes physically interpretable relationship between performance metric and experimental cycle. This renders it intuitive and useful for delineating degradation or forecasting failure. Performance degradation trajectory fundamentally depends on two critical elements: appropriate failure threshold and degradation model. Common failure threshold types for lifting machinery electronics include acquisition accuracy, output accuracy, and linearity, which can be determined based on design specifications and operational requirements. Degradation models are generally consistent across samples, distinctions manifest in parameters α and β .This parametric variability stems from the inherent randomness during sampling, which further induces dispersion in pseudo-lifetime. Consequently, a lifetime distribution model can be established to assess equipment-level reliability.

3.2. Lifetime distribution model

As a representative lifetime distribution model, Weibull is widely applied in reliability studies of electronic components and equipment [39,40], represented by:

$$F(t) = \begin{cases} 1 - exp\left[-\left(\frac{t}{\eta}\right)^m\right] & t \geq 0 \\ 0 & t < 0 \end{cases} \quad (10)$$

where $F(t)$ is cumulative failure distribution function, t is equipment lifespan, and m and η denote shape parameter and scale parameter, respectively. The core advantage of Weibull distribution model lies in its flexible shape and scale parameters, which enable it to fit a wide range of failure patterns and reduce to several well-known distribution forms, such as exponential distribution ($m = 1$) and Rayleigh distribution ($m = 2$) [41].

Suppose the pseudo-lifetimes of test samples obtained based on either the ARMA model or performance degradation trajectory are L_1, L_2, L_3, ... L_s, the combination is written as:

$$L_A = [L_1 \quad L_2 \quad L_3 \quad ... \quad L_s] \quad (11)$$

A lifetime distribution model of lifting machinery electronic equipment is established according to the flow chart illustrated in Fig. 3.

In Fig. 3, Anderson-Darling test is used to validate the conformity of Weibull distribution. Parameters m and η are identified via maximum likelihood estimation, and hypothesis validation is performed by Kolmogorov-Smirnov test. Furthermore, key reliability metrics including mean lifetime, reliability function, and failure probability density function, can be derived through the transformations of Eq. (10). This enables quantitative reliability analysis, thereby revealing how the reliability of electronic equipment evolves over time.

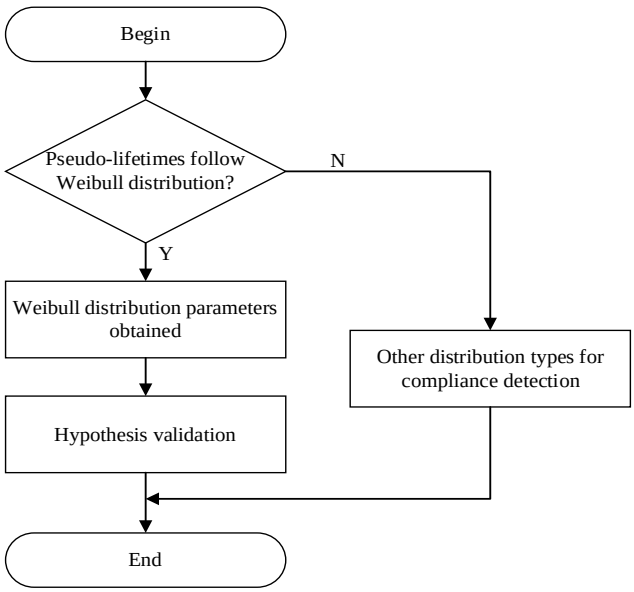

Figure 3. Lifetime distribution modeling flow.

3.3. Reliability assessment procedure

Reliability assessment procedure for lifting machinery electronic equipment can be summarized as follows:

Step 1: ALT and data acquisition

Perform ALT on S samples, $S \geq 4$. Acquire time-series performance data, and record measurement time instants or cycle indices.

Step 2: WP based feature extraction

Decompose, denoise, and reconstruct time series data using WP.

Step 3: Performance degradation trajectory (Eq. 9)

Establish the corresponding relationship between y and $\hat{t}$, after identifying α and β.

Step 4: Pseudo-lifetime calculation (Eq. 8)

Compute pseudo-lifetimes $L_1 \ldots L_s$, according to the performance degradation trajectory and failure threshold.

Step 5: Weibull parameter identification (Fig. 3)

Identify the shape parameter and scale parameter of Weibull distribution model.

Step 6: Quantitative reliability analysis

According to Eq. (10), derive the reliability function, failure probability density function, and mean lifespan, i.e.:

Reliability function

$$R(t) = 1 - F(t) \tag{12}$$

Failure probability density function

$$p(t) = F(t)' \tag{13}$$

Mean lifespan

$$E(t) = \int_0^\infty tp(t)dt \tag{14}$$

4. Case study

4.1. ALT design

LML is the core component of electronic control system in lifting machinery. It automatically interrupts control outputs to enforce safety when detecting dangerous signals such as overload or sensor failure. ALT was designed for four LML samples(named A1, A2, B1, B2) based on Coffin-Manson model, where $c = 2$, $\Delta T_F = 30°C$, $T_{\max} = 80°C$, and $T_{\min} = -40°C$, i.e., the acceleration factor $A_{\mathrm{CM}} = 16$. In Fig. 1, $t_1 = t_2 = 10\ min$, $k = 4°C/min$, i.e., $t_{cycle} = 80\ min$.

4.2. Pseudo-Lifetime calculation

Nominal control output voltage of LML is 24V, with a lower qualified value of 22.8 V, indicating the failure threshold of 1.2 V. Four samples were randomly selected to implement ALT comprising 500 cycles. Time series of output voltage data are established as shown by the dashed line in Fig.4. Variation of the lines reveals that the output voltage exhibits a progressive degradation trend overall, with significant fluctuations and no discernible pattern.

In order to mitigate acquisition errors and data noise, the time series were subjected to WP decomposition using sym8 basis wavelet. The performance degradation curve is depicted by the solid line in Fig. 4 after reconstruction. As shown in Fig. 4, the originally irregular time-series data from the ALT of samples are transformed into smooth and structured degradation trajectories. The underlying degradation trend and characteristics of the output voltage are clearly revealed, demonstrating a significant improvement in data quality. This enhanced signal fidelity provides a solid foundation for subsequent model fitting, degradation pattern analysis, and pseudo-lifetime calculation.

Performance degradation trajectories of the LML samples are fitted using the model Eq. (9), and the identified parameters are summarized in Tab. 1. As shown in Tab. 1, the identified parameters for all samples are closely aligned, indicating a consistent degradation trend across samples. This consistency further corroborates the credibility and repeatability of the ALT data.

Furthermore, we quantitatively compare the goodness-of-fit of Eq. (9) against two alternative models: linear degradation model and power degradation model [42,43]. The results are presented in Tab. 2, where the sum of squared errors (SSE) is adopted as the evaluation metric. A lower SSE indicates better model fit.

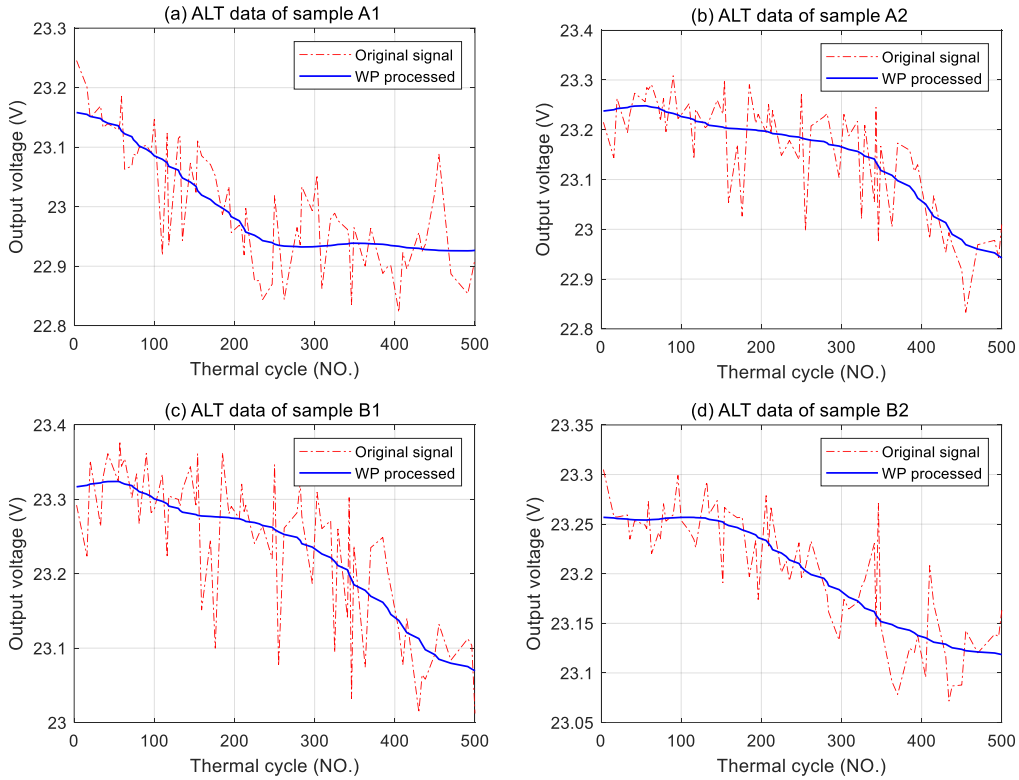

Figure 4. ALT data trends of LML.

Table 1. Identified degradation trajectory parameters of LML samples.

Parameters of Eq. (9)	**A1**	**A2**	**B1**	**B2**
α	-0.1293	-0.3343	-0.4346	-0.3341
β	0.0005	0.0007	0.0007	0.0004

Table 2. Comparison of fitting effects based on the sum of squared errors.

Performance degradation model	**A1**	**A2**	**B1**	**B2**
Eq. (9)	**0.0610**	**0.0597**	**0.0245**	**0.0099**
Linear degradation model ([42,43])	0.0868	0.0726	0.0323	0.0112
Power degradation model ([42,43])	0.0997	0.2495	0.1616	0.0707

Tab. 2 reveals that, for each sample, Eq. (9) consistently outperforms both the linear degradation model and power degradation model in terms of fitting accuracy. Specifically, the average SSE across all samples is reduced by 23.56% compared to the linear model, and by 73.32% relative to the power model. These results support that the degradation trajectory defined in Eq. (9) provides a more accurate and representative characterization of the performance degradation process in electronic equipment.

LML pseudo-lifetime can be calculated using ARMA model or performance degradation trajectory. Taking A1 as an example, the performance degradation trajectory method based on Eq. (9) predicts a failure cycle of 586 (see Fig. 5). As shown in Fig. 5, the fitted degradation trajectory clearly captures the performance degradation patterns. With increasing thermal cycles, the degradation of output voltage follows an exponential growth trend, gradually approaching the failure threshold. Additionally, this degradation trajectory is easily implementable on onboard terminals through programming. ARMA method predicts failure cycle of A1 to be 1340 (see Fig.

6) and $p = 14$, $q = 12$. From Fig. 6, it can be observed that ARMA method also depicts the trend of the output voltage approaching the lower qualified value. However, there exists significant difference between the two methods. The predicted results using the performance degradation trajectory method is notably smaller than that obtained using the ARMA method.

ALT was continued for A1. When the test reached 631 cycles, the performance of A1 irreversibly exceeded the failure threshold (see Fig. 5), resulting in an actual failure cycle of 631. This outcome validates that the prediction based on performance degradation trajectory is accurate. Moreover, the high order and large number of coefficients in ARMA model render it impractical for real-time implementation and embedded deployment. Given the computational and memory constraints of onboard embedded terminals in lifting machinery, the performance degradation trajectory features a simple structure and low computational complexity, thereby meeting the stringent demands of practical engineering deployment.

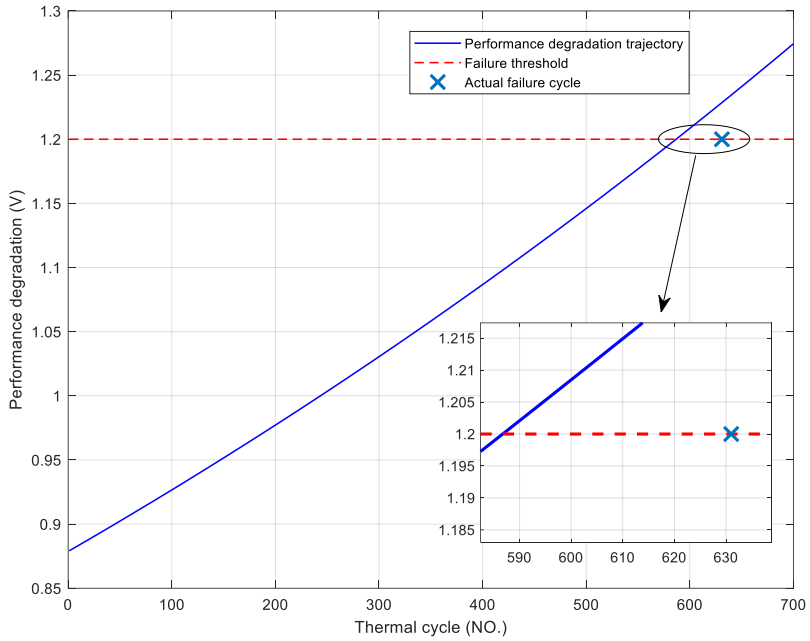

Figure 5. Failure cycles of A1 based on performance degradation trajectory.

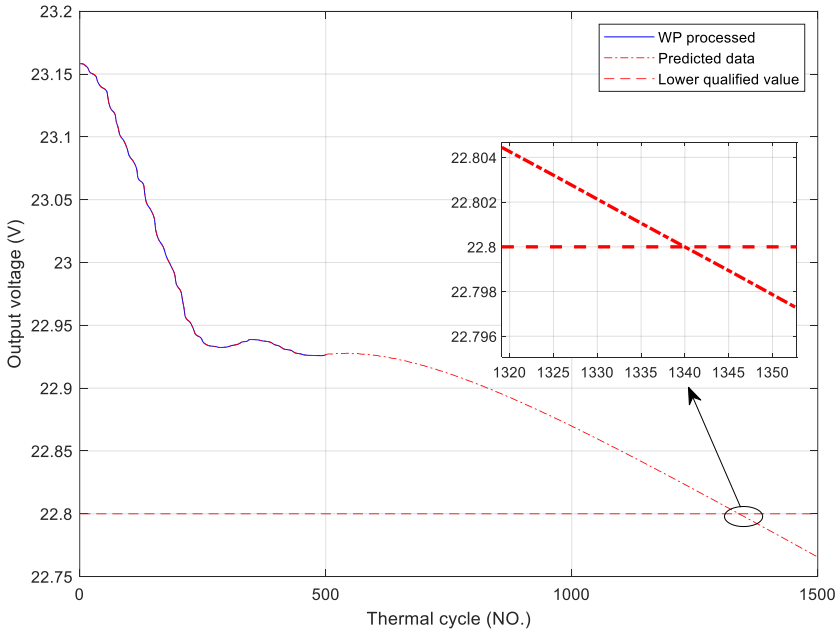

Figure 6. Failure cycles of A1 based on ARMA.

Table 3. Prediction results for all samples based on performance degradation trajectory or ARMA.

Prediction method	A1	A2	B1	B2
Performance degradation trajectory	586	776	920	1181
ARMA	1340	783	986	1462

In the same way, the two methods are used for samples A2, B1, and B2. Comparative results for all samples between both methods are illustrated in Tab. 3. The comparison indicates that the performance degradation trajectory is superior to ARMA as the latter yields markedly conservative estimates. This over-conservatism stems from its reliance on extensive datasets, where reliability data of LML is inherently limited. Therefore, predictive failure cycles of A1, A2, B1, and B2, are identified as 586, 776, 920, and 1181, respectively.

On the basis of Eq. (8), pseudo-lifetimes of A1, A2, B1, and B2 are 12.84, 17.01, 20.16, and 25.88, respectively, i.e.

$$L_A = [12.84 \quad 17.01 \quad 20.16 \quad 25.88]$$

4.3. Reliability assessment

According to the flow chart shown in Fig. 3, the shape parameter and scale parameter are identified as $m = 4.43$ and $\eta = 20.84$, with 95% confidence intervals of [2.05, 9.55] and [16.49, 26.33], respectively. The lifetime distribution model of LML is:

$$F(t) = \begin{cases} 1 - exp\left[-\left(\frac{t}{20.84}\right)^{4.43}\right] & t \geq 0 \\ 0 & t < 0 \end{cases} \tag{16}$$

Furthermore, curves of *R(t)* and $p(t)$ are shown in Fig. 7, with the mean lifetime $E(t) = 19.00$ (in years).

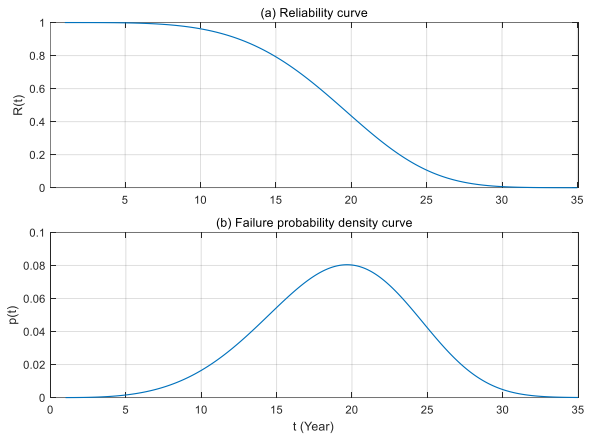

Figure 7. LML reliability and failure probability density curve.

Finally, the quantitative results verify that LML meets the system-level reliability requirements (at least 15 years). The feasibility and accuracy of the methodology are confirmed under the constraints of only four samples and limited data. Notably, lifting machinery users express a pressing need for fault prediction and preventive maintenance of electronic equipment, due to remote and harsh operating environment, coupled with challenging maintenance access. This case demonstrates that the performance degradation trajectory offers intuitive visualization, clear physical interpretability, and ease of algorithm deployment, making it well-suited for lifting machinery.

5. Conclusion

A holistic equipment-level reliability approach is imperative for lifting machinery. Its special-equipment nature and reliability requirements render existing reliability assessment methods unsuitable for onboard electronic equipment. This paper systematically presents a comprehensive methodology, that encompasses ATL, data analysis, and reliability assessment algorithm. An intuitive and cost-effective assessment procedure is also developed to enable rapid deployment.

The LML case study demonstrates that the methodology and procedure are practically feasible. Specifically, the proposed degradation trajectory model achieves superior fitting performance compared to the linear model and power model. The average SSE is reduced by 23.56% and 73.32%, respectively. And, the pseudo-lifetime prediction based on the degradation trajectory also outperforms the ARMA-based approach in terms of accuracy and physical interpretability. The reliability evaluation yields trustworthy quantitative results and reliability curve for LML, which align well with the performance degradation behavior and engineering experience.

The methodology achieves a balance of methodological accuracy and procedural feasibility under small-sample constraints. Owing to the systematic architecture, deployment-friendly design, and quantifiable accuracy, it has promising application in fault prediction, preventive maintenance, and reliability enhancement. Future work will focus on two directions: 1) developing a reliability data acquisition and assessment platform for lifting machinery by integrating the

proposed methodology. 2) exploring a hybrid reliability assessment architecture that synergistically combines physics-based models with data-driven approaches.

Acknowledgment

This work was supported in part by the Jiangsu Provincial Education Science 14th Five-Year Plan Project (C20230125), in part by the Xuzhou Heavy Machinery Technology Project, and in part by the Jiangsu Provincial College Student Innovation Training Program (S202513988006).

References

1. Buffolo M, Favero D, Marcuzzi A, De Santi C, Meneghesso G, Zanoni E. Review and outlook on GaN and SiC power devices: industrial state-of-the-art, applications, and perspectives. IEEE Transactions on Electron Devices 2024; 71(3): 1344–1355. https://doi.org/10.1109/TED.2023.3346369.
2. Mazumder S K, Voss L F, Dowling K M, Conway A, Hall D, Kaplar R J. Overview of wide/ultrawide bandgap power semiconductor devices for distributed energy resources. IEEE Journal of Emerging and Selected Topics in Power Electronics 2023; 11(4): 3957–3982. https://doi.org/10.1109/JESTPE.2023.3277828.
3. Udabe A, Baraia-Etxaburu I, Diez D G. Gallium nitride power devices: a state of the art review. IEEE Access 2023; 11: 48628–48650. https://doi.org/10.1109/ACCESS.2023.3277200.
4. Lai W, Liu A, Wang Z, Shangguan M, Li H, Chen M, Yao R, Xiong Y. Study on lifetime modeling of IGBT modules considering electric frequency influence mechanism. IEEE Transactions on Device and Materials Reliability 2023; 23(3): 395–403. https://doi.org/10.1109/TDMR.2023.3288144.
5. Silva C, Reis G, Alzamora A, Paula H. Reliability analysis of IGBT modules of multilevel inverters operating in hostile mining environments. IEEE Transactions on Industry Applications 2025 ;61(4): 6798–6809. https://doi.org/10.1109/TIA.2025.3546211.
6. Shi Y, Liu J, Ai Y, Chen S, Pei C. Lifetime prediction method of the traction converter IGBT based on plastic strain energy density. IEEE Transactions on Transportation Electrification 2024; 10(1): 1286–1298. https://doi.org/10.1109/TTE.2023.3274567.
7. Lai W, Shangguan M, Shi J, Li H, Wu Y, Yao R, Wang H, Jing H, Li Y. Research on remaining lifetime evaluation for traction system IGBT devices of electric locomotives with different service mileage. IEEE Transactions on Power Electronics 2025; 40(4): 6020–6032. https://doi.org/10.1109/TPEL.2024.3518062.
8. Wang H, Ma J, Yang Y, Gong M, Wang Q. A review of system-in-package technologies: application and reliability of advanced packaging. Micromachines 2023; 14(6): 1149. https://doi.org/10.3390/mi14061149.
9. Guan Q, Hang C, Li S, Zhang X, Liu Y, Wang Z. Research progress on the solder joint reliability of electronics used in deep space exploration. Chinese Journal of Mechanical Engineering 2023; 36(2): 16–28. https://doi.org/10.1186/s10033-023-00834-4.
10. Qiu B, Luo D, Wang Y, Nie X. Failure analysis technology of military electronic package and relevant cases. Environmental Technology 2010; 30(5): 44–49. https://doi.org/10.3969/j.issn.1004-7204.2010.05.011.
11. Wang H, Blaabjerg F. Power electronics reliability: state of the art and outlook. IEEE Journal of Emerging and Selected Topics in Power Electronics 2021; 9(6): 6476–6493. https://doi.org/10.1109/JESTPE.2020.3037161.
12. Peyghami S, Blaabjerg F, Palensky P. Incorporating power electronic converters reliability into modern power system reliability analysis. IEEE Journal of Emerging and Selected Topics in Power Electronics 2021; 9(2): 1668–1681. https://doi.org/10.1109/JESTPE.2020.2967216.
13. Chen Y, Yang T, Wang Y. Reliability modeling of mutual DCFP considering failure physical dependency. Journal of Systems Engineering and Electronics 2023; 34(4): 1063–1073. https://doi.org/10.23919/JSEE.2023.000108.
14. Xu Q, Xu Y, Tu P, Zhao T, Wang P. Systematic reliability modeling and evaluation for on-board power systems of more electric aircrafts. IEEE Transactions on Power Systems 2019; 34(4): 3264–3273. https://doi.org/10.1109/TPWRS.2019.2896454.
15. Rezaei A, Fathollahi A, Akbari E, Saki M. Reliability calculation improvement of electrolytic capacitor banks used in energy storage applications based on internal capacitor faults and degradation. IEEE Access 2024; 12: 13146–13164. https://doi.org/10.1109/ACCESS.2024.3351604.

16. Altamimi A, Jayaweera D. Reliability of power systems with climate change impacts on hierarchical levels of PV systems. Electric Power Systems Research 2021; 190: 106830. https://doi.org/10.1016/j.epsr.2020.106830.
17. Kumar V, Singh K, Tripathi K. Reliability prediction methods for electronic devices: a state-of-the-art review. IETE Technical Review 2022; 39: 460–470. https://doi.org/10.1080/02564602.2020.1843552.
18. Anusuya K, Vijayakumar K. Comparative study of component-level reliability approaches in power electronic components. In: Proceedings of the 3rd International Conference on Advancement in Electrical and Electronic Engineering (ICAEEE); 2024; Gazipur, Bangladesh: IEEE; 1–6. https://doi.org/10.1109/ICAEEE62219.2024.10561767.
19. Novak M, Sangwongwanich A, Blaabjerg F. Monte Carlo-based reliability estimation methods for power devices in power electronics systems. IEEE Open Journal of Power Electronics 2021; 2: 523–534. https://doi.org/10.1109/OJPEL.2021.3116070.
20. Vermelin W, Lövberg A, Misiorny M, Eng M, Brinkfeldt K. Data-driven remaining useful life estimation of discrete power electronic devices. In: Proceedings of the 33rd European Safety and Reliability Conference (ESREL 2023); 2023; Southampton, UK; 2595–2602. https://doi.org/10.3850/978-981-18-8071-1_P561-cd.
21. Peyghami S, Wang Z, Blaabjerg F. A guideline for reliability prediction in power electronic converters. IEEE Transactions on Power Electronics 2020; 35(10): 10958–10968. https://doi.org/10.1109/TPEL.2020.2981933.
22. Tian W, Zha W, Lei H, Yang X. Research and analysis of reliability evaluation methods for automotive electronic components. In: Proceedings of the 25th International Conference on Electronic Packaging Technology (ICEPT); 2024; Tianjin, China: IEEE; 1–4. https://doi.org/10.1109/ICEPT63120.2024.10668438.
23. Shahbazi M, Smith N A, Marzband M, Habib H U R. A reliability-optimized maximum power point tracking algorithm utilizing neural networks for long-term lifetime prediction for photovoltaic power converters. Energies 2023; 16: 6071. https://doi.org/10.3390/en16166071.
24. Wang Z, Ding Y, Han T, Xu Q, Yan H, Xie M. Adaptive attention-driven few-shot learning for robust fault diagnosis. IEEE Sensors Journal 2024; 24(16): 26034–26043. https://doi.org/10.1109/JSEN.2024.3421242.
25. Liu Z, Yang S, Suo B. Storage life prediction of high-voltage diodes based on improved artificial bee colony algorithm optimized LSTM-transformer framework. Electronics 2025; 14(15): 3030. https://doi.org/10.3390/electronics14153030.
26. Aparicio-Téllez R, Garcia-Bosque M, Díez-Señorans G, Celma S. Oscillator selection strategies to optimize a physically unclonable function for IoT systems security. Sensors 2023; 23(9): 4410. https://doi.org/10.3390/s23094410.
27. Zhao S, Makis V, Chen S, Li Y. Health assessment method for electronic components subject to condition monitoring and hard failure. IEEE Transactions on Instrumentation and Measurement 2019; 68(1): 138–150. https://doi.org/10.1109/TIM.2018.2839938.
28. Wang, X, Su, X, Wang, J. Nonlinear doubly wiener constant-stress accelerated degradation nodel based on uncertainties and acceleration factor constant principle. Applied Sciences 2021; 11(19): 8968. https://doi.org/10.3390/app11198968.
29. You D, Liu S, Li F, Liu H, Zhang Y. Reliability assessment method based on small sample accelerated life test data. Eksploatacja i Niezawodność – Maintenance and Reliability 2025; 27(1): 192170. https://doi.org/10.17531/ein/192170.
30. Bhargava C, Sharma P, Senthilkumar M, Padmanaban S, Leonowicz Z. Review of health prognostics and condition monitoring of electronic components. IEEE Access 2020; 8: 75163–75183. https://doi.org/10.1109/ACCESS.2020.2989410.
31. Zhao F, Yuan Y, Chen C, Xiao L. Temperature prediction for electromechanical equipment in open-pit coal mines under complex working conditions using wavelet packet decomposition and graph attention network. Eksploatacja i Niezawodność – Maintenance and Reliability 2025; 27(3): 197381. https://doi.org/10.17531/ein/197381.
32. Song R, Chen W, Wang Y, Du L, Wang P. Transformer aging diagnosis method based on Raman spectroscopy wavelet packet-SPCA feature extraction. IEEE Transactions on Instrumentation and Measurement 2023; 72: 1–8. https://doi.org/10.1109/TIM.2022.3225005.
33. Lu G, Wen X, He G, Yi X, Yan P. Early fault warning and identification in condition monitoring of bearing via wavelet packet decomposition coupled with graph. IEEE/ASME Transactions on Mechatronics 2022; 27(5): 3155–3164. https://doi.org/10.1109/TMECH.2021.3110988.
34. Fang C, Chen Y, Deng X, Lin X, Han Y, Zheng J. Denoising method of machine tool vibration signal based on variational mode decomposition and Whale–Tabu optimization algorithm. Scientific Reports 2023; 13: 1505. https://doi.org/10.1038/s41598-023-28404-7.
35. Chen Y, Xia X, Zhou W, Zhang J, Teng X, Chen Y. Prediction of the Lithium-Ion battery remaining useful life based on EMD-ARMA.

Journal of Electric Power 2021; 36(1): 43–50. https://doi.org/10.13357/j.dlxb.2021.006.

36. Chen C, Wang C, Lu N, Jiang B, Xing Y. A data-driven predictive maintenance strategy based on accurate failure prognostics. Eksploatacja i Niezawodność – Maintenance and Reliability 2021; 23(2): 387–394. https://doi.org/10.17531/ein.2021.2.19.
37. Gonzalez-Rodriguez PS, Lozoya-Santos JdJ, Gonzalez-Hernandez H G, Felix-Herran L C, Tudon-Martinez J C. Challenges and opportunities for extending battery pack life using new algorithms and techniques for battery electric vehicles. World Electric Vehicle Journal 2025; 16(8): 442. https://doi.org/10.3390/wevj16080442.
38. Patrizi G, Martiri L, Pievatolo A, Magrini A, Meccariello G, Cristaldi L, Nikiforova N D. A review of degradation models and remaining useful life prediction for testing design and predictive maintenance of lithium-ion batteries. Sensors 2024; 24(11): 3382. https://doi.org/10.3390/s24113382.
39. Ling H. Optimal designs of multiple step-stress accelerated life tests for one-shot devices with Weibull lifetime distributions. IEEE Transactions on Reliability 2025; 74(3): 3017–3027. https://doi.org/10.1109/TR.2024.3480969.
40. Wang J, Wu J, Zhang J, Zhang Q, Fang Y, Huang X. Remaining useful life prediction method by integrating two-phase accelerated degradation data and field information. IEEE Transactions on Instrumentation and Measurement 2024; 73: 1–17. https://doi.org/10.1109/TIM.2024.3381295.
41. Kolev K, Tanev A. Identifying batch problems in aircraft field reliability analysis. Aerospace Research in Bulgaria 2022; 34: 130–137. https://doi.org/10.3897/arb.v34.e11.
42. Gu Y, Shen Y, Yu D. Degradation reliability analysis based on TOPSIS model selection method. Journal of Shanghai Jiaotong University (Science) 2019; 24(3): 351–356. https://doi.org/10.1007/s12204-019-2067-5.
43. Zhang Y, Yu G, Wang L, Jiang N. Performance degradation data based NC rotary table reliability predictions using a single sample. Journal of Tsinghua University (Science and Technology) 2020; 60(4): 299–305. https://doi.org/10.16511/j.cnki.qhdxxb.2019.22.049.